Theoretical Studies on the Smallest Fullerene: from Monomer to Oligomers and Solid States

Zhongfang Chen,*[a] Thomas Heine,*[c] Haijun Jiao,[d] Andreas Hirsch,[b] Walter Thiel,[e] and Paul von Ragué Schleyer[a]

Abstract: Hybrid B3LYP and density-functional-based tight-binding (DFTB) computations on the solid-state structures and electronic properties of the C_{20} fullerene monomer and oligomers are reported. C_{20} cages with C_2, C_{2h}, C_i, D_{3d}, and D_{2h} symmetries have similar energies and geometries. Release of the very high C_{20} strain is, in theory, responsible for the ready oligomerization and the formation of different solid phases. Open [2+2] bonding is preferred both in the oligomers and in the infinite one-dimensional solids; the latter may exhibit metallic character. Two types of three-dimensional solids, the open [2+2] simple cubic and the body-centered cubic (*bcc*) forms, are proposed. The energy of the latter is lower due to the better oligomer bonding. The open [2+2] simple cubic solid should be a conductor, whereas the *bcc* solids are insulators. The most stable three-dimensional solid-state structure, an anisotropically compressed form of the *bcc* solid, has a HOMO–LUMO gap of approximately 2 eV and a larger binding energy than that of the proposed C_{36} solid.

Keywords: C_{20} · density functional calculations · fullerenes · oligomers · solid-state structures

Introduction

The chemistry of the smaller fullerenes is exemplified by C_{20}, which can form the most basic cage. Consisting solely of condensed, unsaturated pentagons with extreme curvature, this enormously strained fullerene should be very reactive and have only a fleeting existence in the condensed states. C_{20} has been the subject of many investigations. Depending on the sophistication of the theoretical methods employed,[1] ring and bowl C_{20} structures have been computed to be more stable than the cage. Some prior investigations even favored bicyclic rings[2,3] and linear chains.[4] Whatever the C_{20} global minimum may be, the basically dodecahedral fullerene (the focus of our attention here) was confirmed to have the lowest energy among all the mathematically possible 20-vertex trivalent polyhedral cages.[5]

The viability of the C_{20} cage was established experimentally by its gas-phase synthesis; the chemical route employed opens a gateway to new carbon materials.[6] C_{20} was characterized by anion photoelectron spectroscopy[6] and further confirmed by comparison with computed vibronic fine structure[7] and systematic computations of the free energies, electron affinities, and vibrational progressions of more than ten possible isomers.[8] To assist the characterization, the low-energy electron-scattering resonant structures,[9] the optical absorption,[10] IR, Raman, and anion photoelectron[11] spectra, as well as NMR chemical shifts of C_{20} isomers[12] also have been computed.

Moreover, the vibronic coupling of the C_{20} cage should be larger than that of C_{60}. Solids based on C_{20} have been considered as superconductivity candidates.[13] Like C_{36}, whose macroscopic solid-state synthesis has been claimed,[14] C_{20}

[a] Dr. Z. Chen, Prof. Dr. P. v. R. Schleyer
Computational Chemistry Annex
The University of Georgia
Athens, GA 30602-2525 (USA)
E-mail: chen@organik.uni-erlangen.de

[b] Prof. Dr. A. Hirsch
Institut für Organische Chemie
Universität Erlangen–Nürnberg
Henkestrasse 42, 91054 Erlangen (Germany)
Fax: (+49) 9131-85-26864

[c] Dr. T. Heine
Institut für Physikalische Chemie und Elektrochemie
Technische Universität Dresden
Mommsenstrasse 13, 01062 Dresden (Germany)
E-mail: Thomas.Heine@chemie.tu-dresden.de

[d] Dr. H. Jiao
Leibniz-Institut für Organische Katalyse
an der Universität Rostock e.V.
Buchbinderstrasse 5–6, 18055 Rostock (Germany)

[e] Prof. Dr. W. Thiel
Max-Planck-Institut für Kohlenforschung
Kaiser-Wilhelm-Platz 1
45470 Mülheim an der Ruhr (Germany)

Supporting information for this article is available on the WWW under http://www.chemeurj.org/ or from the author. It contains C_{20} structures with different symmetries and relative energies.

 DOI: 10.1002/chem.200305538

cages should also condense into various aggregates. Indeed, solid C_{20} was prepared recently by ion-beam irradiation;[15] C_{20} cages appeared to serve as building blocks in the hexagonal crystals that formed.[15] Computations show that C_{20} cages can condense in different ways; such materials under carrier doping are superconductor candidates.[16] Furthermore, $(C_{20})_k^+$ oligomers ($k=1$–13), formed by coalescence of C_{20} cages, have been identified experimentally.[17] Most recently, the C_{20} [2+2] cycloaddition dimerization mechanism was elucidated theoretically.[18]

This new C_{20} cage building block for organic solids poses many questions. We address some of these by employing hybrid B3LYP density functional and density-functional-based tight-binding (DFTB) computations. What is the most stable structure of the isolated C_{20} cage? How easily does C_{20} condense? What is the most likely solid-state structure of C_{20}? Our goal is to gain deeper insight and to facilitate experimental investigations on these promising materials.

Computational Methods

C_{20} monomer structures were fully optimized in the chosen symmetry and then characterized as mimima by vibrational frequency computations at the B3LYP6-31G* density-functional level. The geometries were recomputed at the electron-correlated MP2/6-31G* level of ab initio theory, also employing the Gaussian 98 suite of programs.[19] The oligomers (Tables 1 and 2 and Figures 2–4 later) were fully optimized with symmetry constraints at the B3LYP6-31G* level. The choice of starting three-dimensional solid-state geometry was based on the preferred bonding of 1) the oligomers as well as one-dimensional chains, and 2) the isostructural cells (i.e., with intercage bonds replacing the C–H addition pattern) of the particularly stable $C_{20}H_8$ molecule (Scheme 1). The final connectivities in the aggregates, that is, the inter- and intracage bonds, depend on the size of the unit cells. DFTB[20] calculations were also performed on oligomers and periodic solid-state structrures. In the latter, geometry optimizations were carried out in unit cells of 40 atoms with 81 k-points per cell ($3\times3\times3$). Both coordinates and cell parameters were fully optimized. The unit cells were enlarged to super cells of 320 atoms for the density-of-states (DOS) calculations and the Γ point approximation was applied.

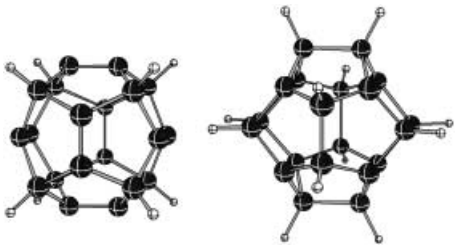

Scheme 1. Structures of $C_{20}H_8$ (T_h) (left) and $C_{20}H_{12}$ (T_h) (right).

Results and Discussion

C_{20} monomer structures: It is well known that the symmetry of cage C_{20} is reduced from the perfect I_h due to Jahn–Teller distortion.[21] However, the lowest energy form of C_{20} is still in doubt. Previous Hartree–Fock (HF) and conventional DFT (local density approximation and the generalized gradient approximation proposed by Perdew, Burke, and Ernzerhof) calculations disagreed on the symmetry of the best geometry (see ref. [22] for a recent review). We computed five possible C_{20} structures with C_2, C_{2h}, C_i, D_{3d}, and D_{2h} point groups at both the B3LYP6-31G* and MP2/6-31G* levels. All were characterized to be true minima by frequency analysis at the B3LYP6-31G* level. The B3LYP6-31G* optimized C_2 structure is shown in Figure 1 (see Supporting Information for the energies and geometries of the other structures). Not only do we find these five isomers to be isoenergetic to within 0.2 kcal mol^{-1} at the B3LYP level (the same is at the MP2 level, except D_{2h}, which is 0.5 kcal mol^{-1} higher in energy than the lowest energy isomer), but they have essentially the same structural parameters at both B3LYP and MP2 levels (see Supporting Information). Hence, we expect the C_{20} cage monomer to be highly fluxional, converting from one structure to another with negligible barriers.

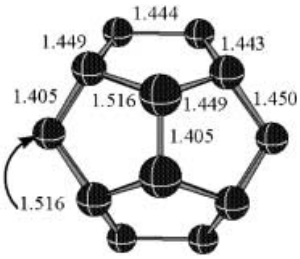

Figure 1. The B3LYP6-31G* optimized structure of C_{20} (C_2). The arrow points to the invisible C–C bond.

The less strained $C_{20}H_8$ (T_h) molecule—building block of the aggregated solids: Graphed theoretically, the presence of eight isolated sp^3 carbons can separate the dodecahedron cage into the six essentially ethylene-like C=C units shown for $C_{20}H_8$ (T_h) in Scheme 1. Its isostructural analogues, $C_{12}N_8$ and $C_{12}P_8$, have been discussed recently.[23] On the basis of isodesmic reactions [Eqs. (1) and (2)], $C_{20}H_8$ (T_h) is less strained than $C_{20}H_{12}$ (T_h). The latter is a spherical homoaromatic system,[24] and also a molecular model for the simple-cubic-like lattice of solid-state C_{20}.[16a] The smaller strain energy in $C_{20}H_8$ (T_h) can also been seen from the energies (per H_2) of the hydrogenation reactions ([Eqs. (3)–(5)]; −67.0, −36.5, and −61.9 kcal mol^{-1} for $C_{20}H_8$, $C_{20}H_{12}$, and $C_{20}H_{20}$, respectively).

$$4\,Me_2C{=}CMe_2 + C_{20}H_{20}(I_h) = 4\,Me_2CH{-}CHMe_2 + C_{20}H_{12}(T_h)$$
$$\Delta H = 273.2\ \text{kcal mol}^{-1} \quad (1)$$

$$6\,Me_2C{=}CMe_2 + C_{20}H_{20}(I_h) = 6\,Me_2CH{-}CHMe_2 + C_{20}H_8(T_h)$$
$$\Delta H = 149.4\ \text{kcal mol}^{-1} \quad (2)$$

$$C_{20} + 4\,H_2 = C_{20}H_8(T_h) \quad \Delta H\ (\text{per } H_2) = -67.0\ \text{kcal mol}^{-1} \quad (3)$$

$$C_{20} + 6\,H_2 = C_{20}H_{12}(T_h) \quad \Delta H\ (\text{per } H_2) = -36.5\ \text{kcal mol}^{-1} \quad (4)$$

$$C_{20} + 10\,H_2 = C_{20}H_{20}(I_h) \quad \Delta H\ (\text{per } H_2) = -61.9\ \text{kcal mol}^{-1} \quad (5)$$

The smaller strain energy in $C_{20}H_8$ (T_h), compared with that in $C_{20}H_{12}$ (T_h), indicates that the solid-state material with the same bonding as in $C_{20}H_8$ (T_h), may be more stable thermodynamically (see the solid-state part).

Dimer structures: Both the singlet and triplet states of five C_{20} dimers were investigated (Table 1 and Figure 2): 1) the closed [2+2] dimer (**1**), in which two cage–cage junction C–C bonds form a four-membered ring; 2) the single-bond dimer (**2**) with only one linking C–C bond; 3) the face-to-face dimer (**3**) with five bonds connecting two neighboring C_{20} molecules; 4) the open [2+2] dimer (**4**) with broken intracage bonds, and 5) the twisted dimer (**5**) with opened C_{20} cages.

Consistent with the results of Choi and Lee,[18] the open [2+2] dimer singlet (**4**) is the lowest energy isomer among all the singlet and triplet alternatives considered; these are approximately 20–88 kcal mol^{-1} less stable, but their dimerization energies are still considerable. The two most stable isomers, **4** and **5**, do not have four-membered rings. The energies of the **1** and **4** triplets are 26.7 and 30.5 kcal mol^{-1}, respectively, higher than the corresponding singlets, but the **2**, **3**, and **5** triplets are 13.3, 5.2, and 8.7 kcal mol^{-1}, respectively, more stable than their singlet forms.

Singlet **4** has the largest HOMO–LUMO gap (2.47 eV), greater than that of the C_{20} monomer (1.95 eV). In contrast, the HOMO–LUMO gap (1.01 eV) of the second-most-stable singlet, **5**, is much smaller. Thus, singlet isomer **4**, with a dimerization energy of 138.2 kcal mol^{-1}, is the most probable dimer structure. Note that the best $(C_{20})_2$ dimer structure (**4**) and its binding energy differ considerably from those of the weakly-bound $(C_{60})_2$,[25] and $(C_{36})_2$[26] (52.8 kcal mol^{-1} at the B3LYP6-31G* level). The following discussion only considers the singlets.

The optimized structures of the dianions are depicted in Figure 2. The addition of two electrons lengthens the interfullerene bonds of all the isomers and changes their stability order. As expected, the open-caged structures, $\mathbf{4}^{2-}$ and $\mathbf{5}^{2-}$, are the two most stable dianions. However, $\mathbf{4}^{2-}$ is 13.7 kcal mol^{-1} higher in energy than $\mathbf{5}^{2-}$.

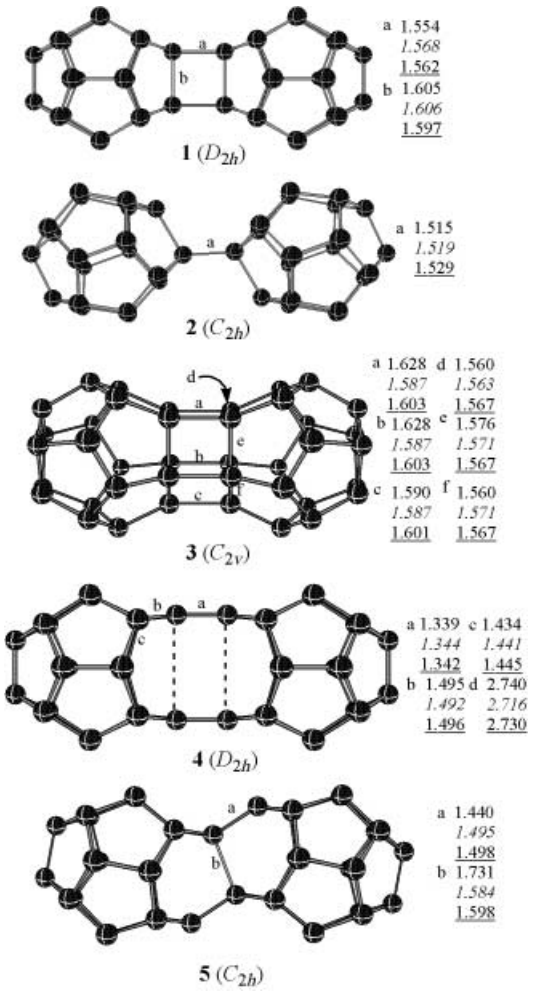

Figure 2. The B3LYP6-31G* optimized structures of $(C_{20})_2$ and its dianion (normal for singlet, italic for triplet, underlined for dianion).

Trimer and tetramer structures: Guided by the experience with the dimers, we can easily imagine chain structures **6**–**10** for the trimer and **11**–**14** for the tetramer. Their optimized geometries are summarized in Figures 3 and 4, respectively, and their energies are given in Table 2. These structures can be extended further into one-dimensional chain polymers. As expected, the open [2+2] trimer **9** has the lowest energy by far; the second most stable isomer **10** (with a twisted open-cage structure) is 55.3 kcal mol^{-1} higher in energy. Moreover, **9** has a larger HOMO–LUMO gap (2.16 eV) than the monomer, whereas the gap for **10** is much smaller (0.45 eV).

Like the dimer and trimer, the linear open [2+2] bonded ladderlike tetramer **13** is approximately 78 kcal mol^{-1} more stable than **14**, and is 104–188 kcal mol^{-1} lower in energy than the other tetramer candi-

Table 1. The B3LYP6-31G* relative energies [E_{rel}, kcal mol^{-1}], HOMO–LUMO gap [eV], binding energies [ΔE, kcal mol^{-1}], vertical ionization potentials [VIP, eV], DFTB relative energies [E_{rel}, kcal mol^{-1}], and HOMO–LUMO gap [eV] of C_{20} dimers (Figure 2).

Species		E_{rel}	Gap [eV]	ΔE	VIP [eV]	E_{rel}[a]	Gap[a] [eV]
C_{20}		–	1.95	–	6.88	–	1.37
$(C_{20})_2$ **1**	singlet[b]	35.5	2.30	102.7	6.84	34.5	1.21
	triplet	62.2	–	76.0	–	–	–
$(C_{20})_2$ **2**	singlet[b]	87.8	0.52	50.4	5.62	59.7	1.08
	triplet	74.5	–	63.7	–	–	–
$(C_{20})_2$ **3**	singlet	75.3	1.11	62.9	6.69	77.7	0.38
	triplet	70.1	–	68.1	–	–	–
$(C_{20})_2$ **4**	singlet[b]	0.0	2.47	138.2	7.01	0.0	1.27
	triplet	30.4	–	107.7	–	–	–
$(C_{20})_2$ **5**	singlet	28.8	1.01	109.4	6.11	5.8	1.03
	triplet	20.1	–	118.1	–	–	–
$(C_{20})_2$ $\mathbf{1}^{2-}$		45.8	–	–	–	–	–
$(C_{20})_2$ $\mathbf{2}^{2-}$		57.6	–	–	–	–	–
$(C_{20})_2$ $\mathbf{3}^{2-}$		28.8	–	–	–	–	–
$(C_{20})_2$ $\mathbf{4}^{2-}$		13.7	–	–	–	–	–
$(C_{20})_2$ $\mathbf{5}^{2-}$		0.0	–	–	–	–	–

[a] at DFTB level. [b] These species have recently been computed at HF/6-31G* (ref. [18]).

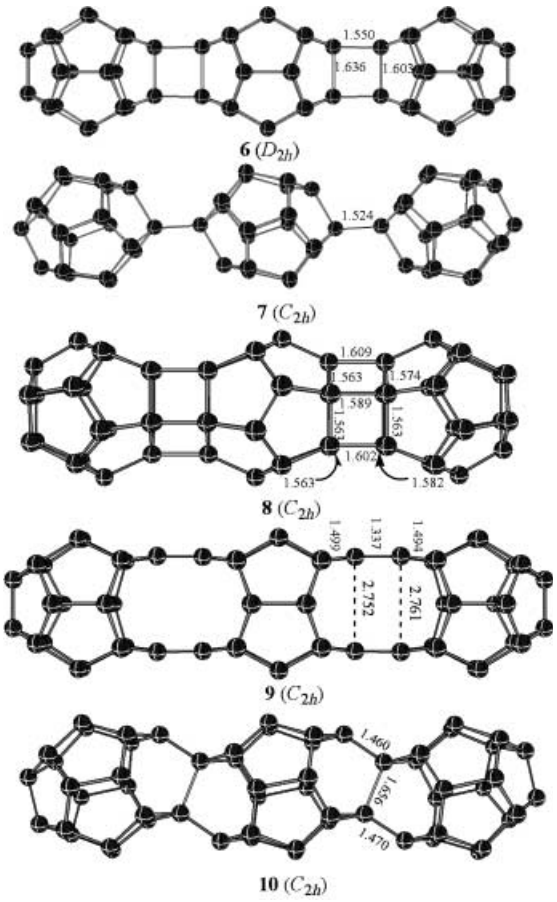

Figure 3. The B3LYP/6-31G* optimized structure of $(C_{20})_3$.

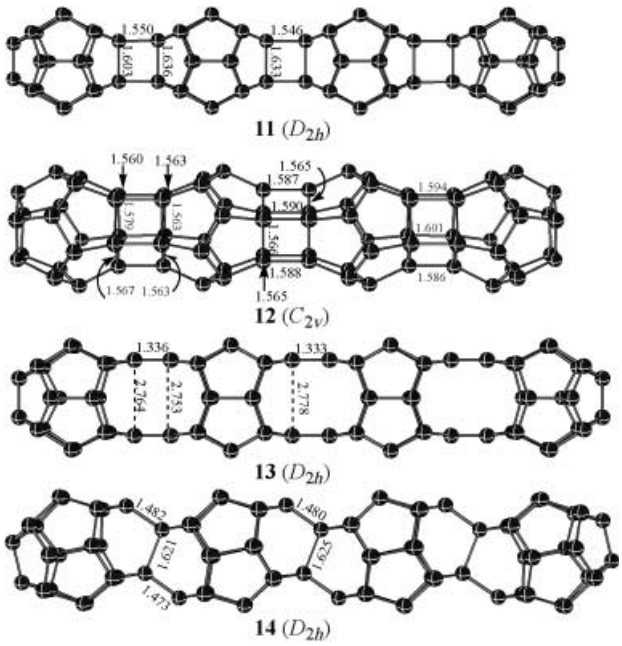

Figure 4. The B3LYP6-31G* optimized structure of $(C_{20})_4$.

dates (Table 2). The high stability of **13**, which suggests that it might be realized experimentally, is due to the absence of unfavorable four-membered rings. This is also true for the twisted open-caged [2+2] bonded tetramer **14**, the second-most-stable tetramer. The lowest energy tetramer, **13**, has a large HOMO–LUMP gap (2.00 eV), whereas the gap for **14** (0.2 eV) is much smaller.

As an aid to characterization, the theoretical vertical ionization potentials (VIP) for the dimers, trimers, and most stable tetramers have been computed (Tables 1 and 2). The VIPs are based on the energy difference between the neutral and the cation, both computed at the optimized neutral geometry. The VIPs of the most stable oligomers are in the 6.49 to 7.01 eV range; the C_{60} VIP is somewhat larger (experimental 7.57 ± 0.01 eV;[27] computed 7.21 eV at B3LYP6-31G*). The VIPs of the next best isomers, the twisted forms, are approximately 1 eV smaller than those of the best forms; this difference might be used to distinguish these two structures experimentally.

Linear structures: DFTB reproduces the DFT relative energy order (see Tables 1 and 2) and has also performed well in investigations of other solid-state forms of carbon,[28] C_{36}-based solids,[26,29] higher fullerenes,[30] and highly reactive mono- and bicyclic carbon structures.[11,31] We employed this less-time-consuming computational method to investigate the infinite C_{20} chains and solids: the most reasonable linear aggregates are connected by open [2+2] bridges, by closed [2+2] bridges, or have twisted structures, as revealed by computations on oligomers. The three chain forms extending from dimers **4**, **5**, and **1** were computed by using DFTB theory with periodic boundary conditions. Four C_{20} units were included in the unit cell resulting in cell sizes with z dimensions exceeding 20 Å, and computations using the Γ point approximation were performed. The c parameter of the unit cell was optimized, while the x and y cell parameters were fixed at 100 Å to avoid spurious interactions.

Local minima were found for the opened [2+2] and the twisted forms. In contrast to Miyamoto and Saito's findings,[16a] the closed [2+2] form transformed into one of the other two isomers (**15** and **16**, Figure 5) during our DFTB optimization of the cell size. The open [2+2] structure **15**

Table 2. The B3LYP6-31G* relative energies [E_{rel}, kcal mol^{-1}], HOMO–LUMO gap [eV], binding energies [ΔE, kcal mol^{-1}], vertical ionization potentials [VIP, eV], DFTB relative energies [E_{rel}, kcal mol^{-1}], and HOMO–LUMO gap [eV] of C_{20} trimers (Figure 3) and tetramers (Figure 4).

Species	Symm	E_{rel}	ΔE	Gap [eV]	VIP [eV]	E_{rel}[a]	Gap[a] [eV]
$(C_{20})_3$ **6**	D_{2h}	69.7	196.5	2.34	6.63	67.7	0.97
$(C_{20})_3$ **7**	C_{2h}	175.1	91.1	0.23	5.27	125.6	1.15
$(C_{20})_3$ **8**	C_{2h}	135.3	130.9	0.42	6.10	143.9	0.07
$(C_{20})_3$ **9**	D_{2h}	0.0	266.2	2.16	6.49	0.0	1.11
$(C_{20})_3$ **10**	C_{2h}	55.3	210.9	0.45	5.47	13.7	0.87
$(C_{20})_4$ **11**	D_{2h}	103.8	290.3	2.21	–	99.9	0.96
$(C_{20})_4$ **12**	C_{2v}	188.1	205.9	0.21	–	198.4	0.65
$(C_{20})_4$ **13**	D_{2h}	0.0	394.0	2.00	6.21	0.0	0.93
$(C_{20})_4$ **14**	C_{2h}	78.3	315.7	0.20	5.19	20.6	0.81

[a] at DFTB level.

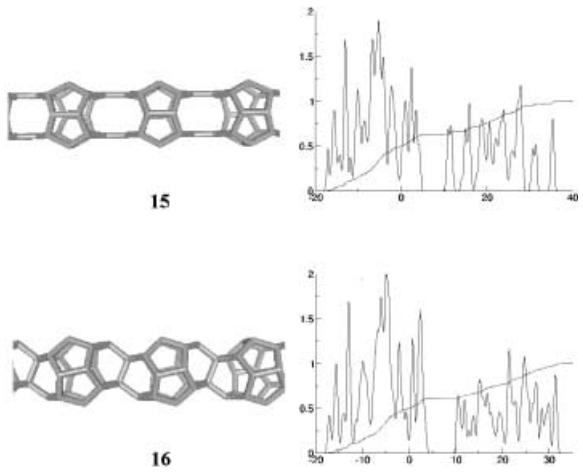

Figure 5. The DFTB-optimized structures and DOS of infinite chains of C_{20}: an open [2+2] chain (**15**) and a twisted chain (**16**).

has a *c* parameter of 5.70 Å per C_{20} unit; this value is 5.50 Å per C_{20} for the twisted structure **16**. The energy of the open [2+2] form **15** is 0.27 eV per C_{20} lower than the twisted form **16** (see Table 3, in which the energies of other forms of carbon are also given for comparison). The electronic structures of **15** and **16** are very similar: neither have a gap at the Fermi level, but have a low density-of-states (DOS) at this Fermi level (Figure 5). There is a gap of approximately 5 eV above the Fermi energy. Thus, these forms should exhibit metallic character; one-dimensional conduction is possible.

Table 3. DFTB binding energies (with respect to the free, spherical, closed-shell atoms) for C_{20} solids and other carbon materials.

Structure	DFTB binding energy [eVatom^{-1}]	Density [g cm^{-3}]	Saturation[d]
diamond	9.22[a]	3.15–3.513[c]	100 %
graphite	9.24[a]	1.9–2.3[c]	0 %
C_{60}	8.85[a]	–	0 %
C_{36} monomer	8.51[b]	–	0 %
C_{36} hexagonal solid	8.67[b]	1.720	33.3 %
C_{20} monomer	8.01	–	0 %
C_{20} open [2+2] chain (**15**)	8.27	–	20 %
C_{20} twisted chain (**16**)	8.25	–	0 %
3D C_{20} solid (**I**)	8.48	2.494	0 %
3D C_{20} solid (**II**)	8.53	2.443	40 %
3D C_{20} solid (**III**)	8.70	2.911	50 %
3D C_{20} solid (**IV**)	8.60	2.803	80 %
3D C_{20} solid (**V**)	8.59	2.844	60 %
3D C_{20} solid (**VI**)	8.67	2.862	70 %

[a] From ref. [28]. [b] From ref. [26]. [c] Experimental. [d] The degree of saturation is the percentage of saturated versus the total number of carbons.

Three-dimensional solid-state structures: Since many three-dimensional solid-state topologies can be formed by aggregation of C_{20} units, we only investigated the most reasonable possibilities. These were based on our experience with the C_{20} oligomers and from previous calculations on C_{20}[16] and C_{36} solids.[26,29,32] The first group of three related candidates were derived from the linear oligomer structures discussed above: the opened (**I**), closed, and half-opened [2+2] bridged structures. The simple cubic (SC) lattice configuration based on the closed structure was studied in Miyamoto and Saito's first paper on C_{20}.[16a] However, in agreement with their later work,[16b] the closed structure is much less stable than other alternatives. DFTB optimization of the unit cell opens the [2+2] bridge. Furthermore, the half-opened form is stabilized further by transformation into the more stable opened [2+2]-bridged structure. Consequently, the latter was the only form we investigated further in this first SC group. (Twisted chain extensions require large tilts of the C_{20} units and are therefore not realistic.)

The second group is based on the extraordinarily stable $C_{20}H_8$ isomer, whose "$C_{20}H_8$–8H" cage is used as the building block. When these units are joined by transforming the C–H bonds into intercage C–C bonds, a body-centered cubic (*bcc*) structure (**II**) is created. Within the *bcc* lattice, no stable structure with additional intercage bonds was found in our computations. However, introducing anisotropy, as suggested earlier,[16b] does lead to the formation of such bonds, either in one- or in two-dimensions (see Figure 6), and consequently considerable further stabilization of the solid (see Table 3). These bonds are [2+2] bridges at the same positions as for the SC solid, which may open with changing the cell size. By employing this technique various new structures can be found, depending on the intercage linkages and the degree of anisotropy introduced into the solid. Four of them, **III**–**VI**, have been considered in our study. All of them have similar binding energies, at least half of their carbons are tetracoordinate, and their densities are approximately 2.8–2.9 g cm^{-3} (see Table 3). Such high densities are similar to that of a C_{22} solid-state structure, proposed recently by Spagnoletti et al.[16c]

One of these structures, **IV**, has been studied earlier by Okada et al.[16b] It has [2+2] bridges in two layers (*xz* and *yz* in our orientation, see Figure 6d). These bridges are arranged in an alternating way: for example in the *xz* plane, [2+2] bridges connect cages in the *z* direction in one layer. At the next layer the [2+2] bridges connect cages in the *x* direction. The analogous arrangement is also found in the *yz* plane. This structure (**IV**) is very stable, in agreement with a previous finding.[16b] Its binding energy is 8.6 eV per carbon atom, only 0.25 eV per carbon atom less than in C_{60}. 80 % of the carbons in **IV** are tetracoordinate (saturated); its density, 2.8 g cm^{-3}, is much higher than that of graphite and approaches the diamond value (~3.15 g cm^{-3}).

We have found two structures even more stable than **IV**. The most stable of these, **III**, contains both small planar sp^2 areas and cagelike sp^3 regions (see Figure 6c); the tetracoordinate carbon content is relatively low (50 %). As a consequence, **III** has a binding energy of 8.7 eV carbon^{-1} (see Table 3) and the highest density (2.91 g cm^{-2}) among all the C_{20}-based solids we studied. The bond lengths, including those of intercage connections, are unexceptional and range

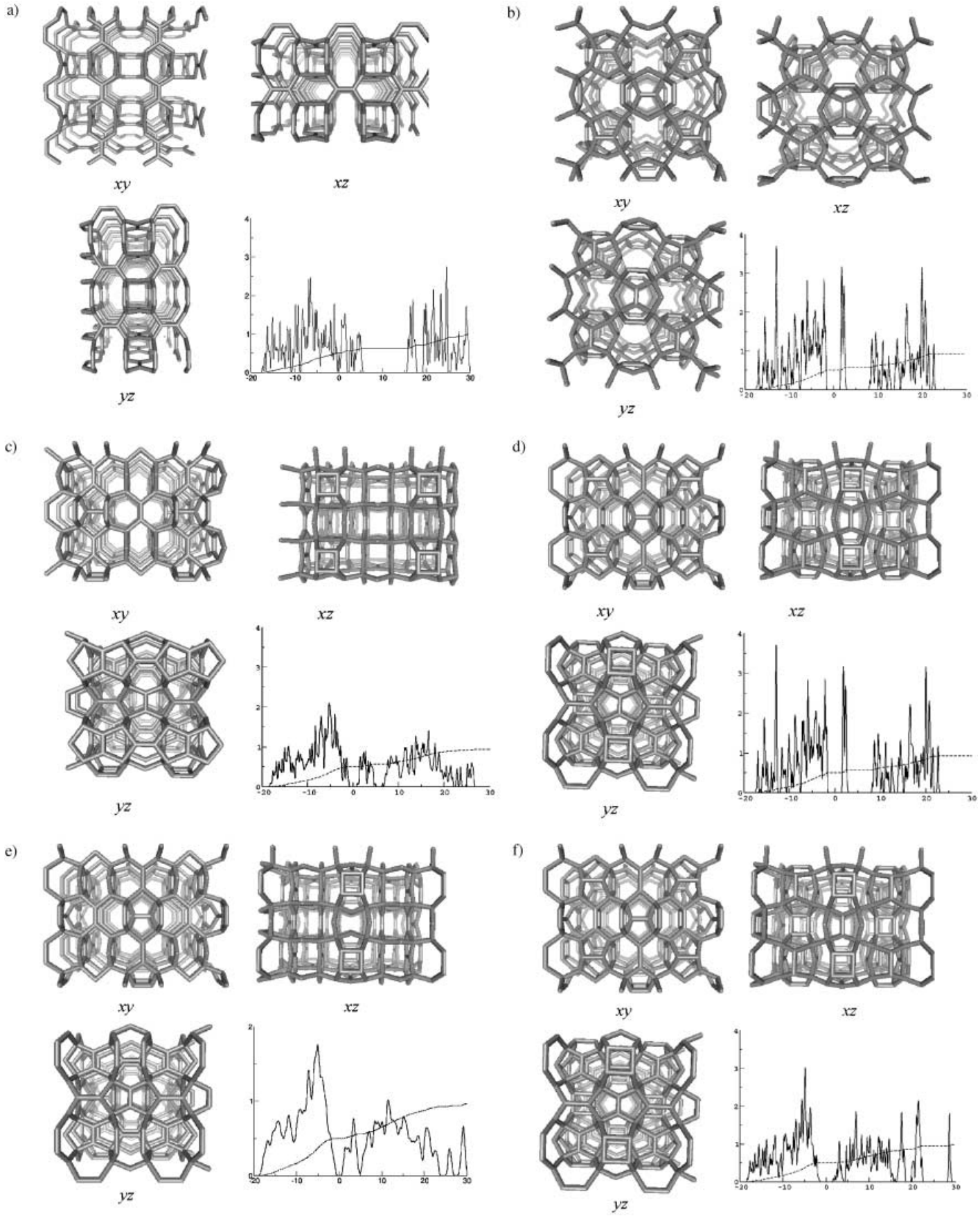

Figure 6. The DFTB-optimized structures and DOS of three-dimensional C_{20} solids: a)–f) are for solids **I**–**VI**, respectively.

from 1.34 Å for the sp^2–sp^2 bonds to 1.55 Å for the sp^3–sp^3 bonds.

Extrapolation of the above approach to a fully saturated *bcc* structure with [2+2] bridges in each spatial direction for every C_{20} unit was unsuccessful. In the recently described hexagonal crystal,[15] C_{20} units act as building blocks. The intermolecular bond length is about 1.5 Å, as expected from strong, covalent bonding. The hexagonal symmetry shown by the electron diffraction pattern[15] is consistent with structures **II**–**VI**. Note that **III**–**VI** were derived from the *bcc* solid-state form, **II**.

So far, no direct experimental X-ray structure determination of the C_{20} solid has been reported. The electronic density-of-states (DOS) of solid-state C_{36} has been measured recently by scanning tunneling spectroscopy.[32a] This technique, which could also be carried out on the C_{20} solid, requires only small amounts of material deposited on a surface.

To assist future experimental investigations, we computed DOS for C_{20} solids discussed here. Only **I** had metallic character (see Figure 6a) due to its small DOS at the Fermi level. At higher energy (6 eV above the Fermi level) it has a remarkably large gap of 10 eV. The *bcc* structure **II** shows its insulating character clearly: its 3.5 eV gap is quite large (Figure 6b) and its DOS has a strong, characteristic peak ~ 1.7 eV above the Fermi level. The DOS's of **III**–**VI** are related to **II**, except that their anisotropy smears the DOS considerably. In particular, the sharp peak of **II** is broadened considerably in **III**–**VI**. Evidently, these states belong to the π bonds of the C_2 units (**II**), or, in **III**–**VI**, by the [2+2] intercage bonds (and remaining C_2 units). In **III** and **IV**, the DOS above the Fermi level is split into two major parts. In all cases besides the "best" structure **III**, for which both parts are comparable, the higher-energy DOS is significantly denser than the lower energy part. In **III**–**VI** the gap is reduced to ~2 eV.

Conclusion

The geometries and energies of C_{20} fullerene minima with different symmetries are nearly the same. Consistent with the recent synthesis of a solid C_{20} crystallite,[15] C_{20} is computed to be very reactive, even more than C_{36}, and forms solid phases with different dimensions easily. The relative stabilities of C_{20} oligomers and solids depend primarily on their strain energies. The thermodynamically most favorable structures of linear oligomers are linked by cyclic C_4 units formed through a [2+2] cycloaddition with subsequent ring opening. The corresponding linear aggregate should exhibit metallic character. Two stable three-dimensional solids, open [2+2] simple cubic and body-centered cubic (*bcc*) forms, are proposed. As expected from the preferred bonding of the oligomers and the maximum strain-energy release principle, the *bcc* form is more thermodynamically stable. The open [2+2] simple cubic solid should be a conductor, whereas the *bcc* solids are insulators. The most stable solid structure, **III**, can be viewed as an anisotropically compressed form of the standard *bcc* solid. The HOMO–LUMO gap of **III** is ~2 eV and its binding energy is greater than that of the proposed C_{36} solid. Our computed DOS might assist the characterization of **III**.

Acknowledgement

We thank the University of Georgia, National Science Foundation Grant CHE-0209857, the Deutsche Forschungsgemeinschaft (DFG/Erlangen) (DFG/Dresden), and the Framework program 6 of the European community (FP6/Dresden) for financial support. Z.C. thanks the Alexander von Humboldt Foundation for a Fellowship, Dr. Weixue Li for helpful discussions, and Prof. Matthias Scheffler for his hospitality in the Fritz-Haber-Institut.

[1] a) V. Parasuk, J. Almlöf, *Chem. Phys. Lett.* **1991**, *184*, 187; b) C. J. Brabec, E. B. Anderson, B. N. Davidson, S. A. Kajihara, Q.-M. Zhang, J. Bernholc, D. Tomanek, *Phys. Rev. B* **1992**, *46*, 7326; c) Z. Slanina, L. Adamowicz, *Thermochim. Acta* **1992**, *23*, 299; d) K. Raghavachari, D. L. Strout, G. K. Odom, G. E. Scuseria, J. A. Pople, B. G. Johnson, P. M. W. Gill, *Chem. Phys. Lett.* **1993**, *214*, 357; e) Z. Slanina, L. Adamowicz, *Fullerene Sci. Technol.* **1993**, *1*, 1; f) M. Sawtarie, M. Menon, K. R. Subbaswamy, *Phys. Rev. B* **1994**, *49*, 7739; g) P. R. Taylor, E. Bylaska, J. H. Weare, R. Kawai, *Chem. Phys. Lett.* **1995**, *235*, 558; h) J. C. Grossman, L. Mitas, K. Raghavachari, *Phys. Rev. Lett.* **1995**, *75*, 3870; i) Z. Wang, P. Day, R. Pachter, *Chem. Phys. Lett.* **1996**, *248*, 121; j) J. M. L. Martin, J. El-Yazal, J.-P. Francois, *Chem. Phys. Lett.* **1996**, *248*, 345; k) E. J. Bylaska, P. R. Taylor, R. Kawai, J. H. Weare, *J. Phys. Chem.* **1996**, *100*, 6966; l) R. O. Jones, G. Seifert, *Phys. Rev. Lett.* **1997**, *79*, 443; m) R. B. Murphy, R. A. Friesner, *Chem. Phys. Lett.* **1998**, *288*, 403; n) S. Sokolova, A. Lüchow, J. B. Anderson, *Chem. Phys. Lett.* **2000**, *323*, 229; o) S. Grimme, C. Mück-Lichtenfeld, *ChemPhysChem* **2002**, *3*, 207; p) M. Saito, Y. Miyamoto, *Phys. Rev. B* **2002**, *65*, 165434; q) K. A. Beran, K. R. Greene, *J. Comput. Chem.* **2002**, *23*, 938; r) K. A. Beran, *J. Comput. Chem.* **2003**, *24*, 1287.

[2] a) G. V. Helden, M. T. Hsu, N. G. Gotts, P. R. Kemper, M. T. Bowers, *Chem. Phys. Lett.* **1993**, *204*, 15; b) J. N. Hunter, J. L. Fey, M. F. Jarrold, *J. Phys. Chem.* **1993**, *97*, 3460; J. N. Hunter, J. L. Fey, M. F. Jarrold, *Science* **1993**, *260*, 784; c) S. Yang, K. J. Taylor, M. J. Craycraft, J. Conceicao, C. L. Pettiette, O. Cheshnovsky, R. E. Smaley, *Chem. Phys. Lett.* **1988**, *144*, 431.

[3] H. Handschuh, G. Ganteför, B. Kessler, P. S. Bechthold, W. Eberhardt, *Phys. Rev. Lett.* **1995**, *74*, 1095.

[4] A. K. Ott, G. A. Rechtsteiner, C. Felix, O. Hampe, M. F. Jarrold, R. P. V. Duyne, K. Raghavachari, *J. Chem. Phys.* **1998**, *109*, 9652.

[5] M. C. Domene, P. W. Fowler, D. Mitchell, G. Seifert, F. Zerbetto, *J. Phys. Chem. A* **1997**, *101*, 8339.

[6] H. Prinzbach, A. Weller, P. Landenberger, F. Wahl, J. Worth, L. T. Scott, M. Gelmont, D. Olevano, B. von Issendorff, *Nature* **2000**, *407*, 60.

[7] M. Saito, Y. Miyamoto, *Phys. Rev. Lett.* **2001**, *87*, 035503.

[8] J. Lu, S. Re, Y. Choe, S. Nagase, Y. Zhou, R. Han, L. Peng, X. Zhang, X. Zhao, *Phys. Rev. B* **2003**, *67*, 125415.

[9] F. A. Gianturco, G. Y. Kashenock, R. R. Lucchese, N. Sanna, *J. Chem. Phys.* **2002**, *116*, 2811.

[10] A. Castro, M. A. L. Marques, J. A. Alonso, G. F. Bertsch, K. Yabana, A. Rubio, *J. Chem. Phys.* **2002**, *116*, 1930.

[11] M. Saito, Y. Miyamoto, *Phys. Rev. B* **2002**, *65*, 165434.

[12] A. H. Romero, D. Sebastiani, R. Ramírez, M. Kiwi, *Chem. Phys. Lett.* **2002**, *366,* 134.

[13] A. Devos, M. Lannoo, J. *Phys. Rev. B.* **1998**, *58*, 8236.

[14] C. Piskoti, J. Yarger, A. Zettl, *Nature* **1998**, *393*, 771.

[15] a) Z. Wang, X. Ke, Z. Zhu, F. Zhu, M. Ruan, H. Chen, R. Huang, L. Zheng, *Phys. Lett. A* **2001**, *280*, 351; b) Z. Wang, X. Ke, Z. Zhu, F. Zhu, W. Wang, G. Yu, M. Ruan, H. Chen, R. Huang, L. Zheng, *Wuli Xuebao* **2000**, *49*, 939.

[16] a) Y. Miyamoto, M. Saito, *Phys. Rev. B* **2001**, *63*, 161401; b) S. Okada, Y. Miyamoto, M. Saito, *Phys. Rev. B* **2001**, *64*, 245405; c) I.

Spagnolatti, M. Bernasconi, G. Benedek, *Europhys. Lett.* **2002**, *59*, 572; Corrigendum: I. Spagnolatti, M. Bernasconi, G. Benedek, *Europhys. Lett.* **2002**, *60*, 329.
[17] R. Ehlich, P. Landenberger, H. Prinzbach, *J. Chem. Phys.* **2001**, *115*, 5830.
[18] C. H. Choi, H. I. Lee, *Chem. Phys. Lett.* **2002**, *359*, 446.
[19] *Gaussian 98*, Revision A.11, M. J. Frisch, G. W. Trucks, H. B. Schlegel, G. E. Scuseria, M. A. Robb, J. R. Cheeseman, V. G. Zakrzewski, J. A. Montgomery, Jr., R. E. Stratmann, J. C. Burant, S. Dapprich, J. M. Millam, A. D. Daniels, K. N. Kudin, M. C. Strain, O. Farkas, J. Tomasi, V. Barone, M. Cossi, R. Cammi, B. Mennucci, C. Pomelli, C. Adamo, S. Clifford, J. Ochterski, G. A. Petersson, P. Y. Ayala, Q. Cui, K. Morokuma, D. K. Malick, A. D. Rabuck, K. Raghavachari, J. B. Foresman, J. Cioslowski, J. V. Ortiz, B. B. Stefanov, G. Liu, A. Liashenko, P. Piskorz, I. Komaromi, R. Gomperts, R. L. Martin, D. J. Fox, T. Keith, M. A. Al-Laham, C. Y. Peng, A. Nanayakkara, C. Gonzalez, M. Challacombe, P. M. W. Gill, B. G. Johnson, W. Chen, M. W. Wong, J. L. Andres, M. Head-Gordon, E. S. Replogle, J. A. Pople, Gaussian, Inc., Pittsburgh PA, **1998**.
[20] a) For review see: T. Frauenheim, G. Seifert, M. Elstner, Z. Hajnal, G. Jungnickel, D. Porezag, S. Suhai, R. Scholz, *Phys. Status Solidi B* **2000**, *217*, 41; C. M. Goringe, D. R. Bowler, E. Hernández, *Rep. Prog. Phys.* **1997**, *60*, 1447; b) D. Porezag, T. Frauenheim, T. Köhler, G. Seifert, R. Kaschner, *Phys. Rev. B* **1995**, *51*, 12947; c) T. Frauenheim, F. Weich, T. Köhler, S. Uhlmann, D. Porezag, G. Seifert, *Phys. Rev. B* **1995**, *52*, 11492; d) G. Seifert, D. Porezag, T. Frauenheim, *Int. J. Quantum Chem.* **1996**, *58*, 185; e) M. Elstner, D. Porezag, G. Jungnickel, J. Elsner, M. Haugk, T. Frauenheim, S. Suhai, G. Seifert, *Phys. Rev. B* **1998**, *58*, 7260.
[21] A. Hirsch, Z. Chen, H. Jiao, *Angew. Chem.* **2000**, *112*, 4079; *Angew. Chem. Int. Ed.* **2000**, *39*, 3915.
[22] G. Galli, F. Gygi, J. C. Golaz, *Phys. Rev. B* **1998**, *57*, 1860, and references therein.
[23] R. W. Alder, J. N. Harvey, P. von R. Schleyer, D. Moran, *Org. Lett.* **2001**, *3*, 3233.
[24] Z. Chen, H. Jiao, A. Hirsch, P. von R. Schleyer, *Angew. Chem.* **2002**, *114*, 4485; *Angew. Chem. Int. Ed.* **2002**, *41*, 4309.
[25] a) G. W. Wang, K. Komatsu, Y. Murata, M. Shiro, *Nature* **1997**, *387*, 583; b) K. Komatsu, G. W. Wang, Y. Murata, T. Tanaka, K. Fujiwara, K. Yamamoto, M. Saunders, *J. Org. Chem.* **1998**, *63*, 9358.
[26] T. Heine, P. W. Fowler, G. Seifert, *Solid State Commun.* **1999**, *111*, 19.
[27] R. K. Yoo, B. Ruscic, J. Berkowitz, *J. Chem. Phys.* **1992**, *96*, 911.
[28] D. Porezag, T. Frauenheim, T. Köhler , G. Seifert, R. Kaschner, *Phys. Rev. B* **1995**, *51*, 12947.
[29] P. W. Fowler, D. Mitchell, F. Zerbetto, *J. Am. Chem. Soc.* **1999**, *121*, 3218.
[30] a) O. V. Boltalina, I. N. Ioffe, L. N. Sidorov, G. Seifert, K. Vietze, *J. Am. Chem. Soc.* **2000**, *122*, 9745; b) T. Heine, F. Zerbetto, G. Seifert, P. W. Fowler, *J. Phys. Chem. A* **2000**, *104* , 3865.
[31] T. Heine, F. Zerbetto, *Chem. Phys. Lett.* **2002**, *358*, 359.
[32] a) P. G. Collins, J. C. Grossman, M. Cote, M. Ishigami, C. Piskoti, S. G. Louie, M. L. Cohen, A. Zettl, *Phys. Rev. Lett.* **1999**, *82*, 165; b) P. W. Fowler, T. Heine, K. M. Rogers, J. P. B. Sandall, G. Seifert, F. Zerbetto, *Chem. Phys. Lett.* **1999**, *300*, 369; c) M. Cote, J. C. Grossman, M. L. Cohen, S. G. Louie, *Phys. Rev. Lett.* **1998**, *81*, 697; d) J. C. Grossman, M. Cote, S. G. Louie, M. L. Cohen, *Chem. Phys. Lett.* **1998**, *284*, 344; e) J. C. Grossman, S. G. Louie, M. L. Cohen, *Phys. Rev. B* **1999**, *60*, 6941; f) M. Menon, E. Richter, *Phys. Rev. B* **1999**, *60*, 13322; g) M. Menon, E. Pichter, *Phys. Rev. B* **1999**, *60*, 13322; h) M. Menon, E. Richter, L. Chernozatonskii, *Phys. Rev. B* **2000**, *62*, 15420; i) E. Burgos, E. Halac, H. Bonadeo, *Chem. Phys. Lett.* **2000**, *320*, 14; j) Y. Huang, Y. Chen, R. Liu, *J. Phys. Chem. Solids* **2000**, *61*, 1475.

Received: September 11, 2003 [F5538]